◆ Human Brain Mapping 28:394–408(2007) ◆

Functional Neural Circuits for Mental Timekeeping

Michael C. Stevens,[1,2*] Kent A. Kiehl,[1–3] Godfrey Pearlson,[1,2] and Vince D. Calhoun[1,2]

[1]*Olin Neuropsychiatry Research Center, Hartford, Connecticut*
[2]*Department of Psychiatry, Yale University School of Medicine, New Haven, Connecticut*
[3]*Department of Psychology, Yale University School of Medicine, New Haven, Connecticut*

Abstract: Theories of mental timekeeping suggest frontostriatal networks may mediate performance of tasks requiring precise timing. We assessed whether frontostriatal networks are functionally integrated during the performance of timing tasks. Functional magnetic resonance imaging (fMRI) data from 31 healthy adults were collected during performance of several different types of discrete interval timing tasks. Independent component analysis (ICA) was used to examine functional connectivity within frontostriatal circuits. ICA identifies groups of spatially discrete brain regions sharing similar patterns of hemodynamic signal change over time. The results confirm the existence of a frontostriatal neural timing circuit that includes anterior cingulate gyrus, supplementary motor area, bilateral anterior insula, bilateral putamen/globus pallidus, bilateral thalamus, and right superior temporal gyrus and supramarginal gyrus. Several other distinct neural circuits were identified that may represent the neurobiological substrates of different information processing stages of mental timekeeping. Small areas of right cerebellum were engaged in several of these circuits, suggesting that cerebellar function may be important in, but not the primary substrate of, the mental timing tasks used in this experiment. These findings are discussed within the context of current biological and information processing models of neural timekeeping. *Hum Brain Mapp 28:394–408, 2007.*

Key words: independent component analysis; network; timing; brain; MRI; syncopate; synchronize

INTRODUCTION

The ability to track the passage of time is important for numerous cognitive processes that plan, execute, and coordinate complex behavior. Neurobiological theories of mental timekeeping propose that mental and motor timing engage one or more networks of distributed brain regions [Gibbon et al., 1997; Rammsayer, 1999; Macar et al., 2002; Lewis and Miall, 2003; MacDonald and Meck, 2004; Meck and Malapani, 2004; Rubia and Smith, 2004; Buhusi and Meck, 2005; Lustig et al., 2005]. It is possible that particular brain structures have different functional roles depending on contextual demands, such as the length of measured intervals or the use of movement to define timekeeping [Lewis and Miall, 2003]. These theories are supported by numerous functional magnetic resonance imaging (fMRI) and positron emission tomography (PET) studies that observe neural activity when time reproduction, estimation, or discrimination is required [Blinkenberg et al., 1996; Sadato et al., 1996; Lejeune et al., 1997; Rao et al., 1997; Wessel et al., 1997; Jancke et al., 1998, 2000; Menon et al., 1998; Rubia et al., 1998, 2000; Mima et al., 1999; Kawashima et al., 2000; Macar et al., 2002; Mayville et al., 2002; Riecker et al., 2003; Ward and Frackowiak, 2003; Coull et al., 2004; Hinton and Meck, 2004; Jantzen et al., 2004]. The brain regions activated during these

*Correspondence to: Michael C. Stevens, Olin Neuropsychiatry Research Center, Whitehall Building, Institute of Living/Hartford Hospital, Hartford, CT 06106. E-mail: msteven@harthosp.org

Received for publication 27 September 2005; Accepted 10 March 2006

DOI: 10.1002/hbm.20285

Published online 30 August 2006 in Wiley InterScience (www.interscience.wiley.com).

tasks include sensorimotor, lateral premotor, and supplementary motor, dorsolateral prefrontal, insula, anterior cingulate cortices, superior temporal gyrus, right parietal lobe, the cerebellum, basal ganglia structures, and the thalamus [see reviews by Macar et al., 2002; Lewis and Miall, 2003; Rubia and Smith, 2004; Buhusi and Meck, 2005]. Of these, frontostriatal brain regions [Gibbon et al., 1997; Meck and Benson, 2002; Ferrandez et al., 2003; Coull et al., 2004; Hinton and Meck, 2004; Pouthas et al., 2005] and the cerebellum [Gibbon et al., 1997; Ivry and Spencer, 2004; but see Harrington et al., 2004] have been proposed to be the most likely primary neural substrates of mental timekeeping.

Few studies have examined whether these brain regions form distinct functionally integrated neural circuits. The identification and characterization of such circuits may help elucidate the neural substrates of mental timekeeping operations. For example, one previous study found that hemodynamic activity was correlated between basal ganglia (putamen and globus pallidus) and thalamus during a cued complex motor sequence task [Menon et al., 2000]. Using magnetoencephalography measurements obtained during finger tapping paced by auditory cues, Pollok et al. [2005] found that activity in sensorimotor cortex was functionally integrated with premotor, supplementary motor, posterior parietal cortex, thalamus, and cerebellum ipsilateral to the response hand. Moritz et al. [2000, 2005] examined which brain regions were functionally correlated to primary motor cortex during simple motor or self-paced tapping. Both tasks showed connectivity between bilateral sensorimotor areas, but only self-paced tapping engaged supplementary motor area cortex with bilateral sensorimotor areas [Moritz et al., 2005]. Although these studies reveal brain regions that are correlated with motor function, the methods used were unable to identify coherent neural networks whose activity might be related to nonmotor timekeeping processes. Neural activity in such networks might not be directly coupled to primary motor cortex activity. In addition, none of these studies examined how functional network activity corresponded to different contextual demands on timing. Therefore, there is need for studies that not only confirm the spatial structure of putative mental timekeeping neural networks, but also studies that link activity in these networks to specific timing task demands.

Data-driven analytic techniques that identify and characterize coherent patterns of coordinated neural activation in different brain regions can address these questions. PET and fMRI neuroimaging data analytic methods typically use the general linear model (GLM) [Friston et al., 1995] to identify and quantify neural activity associated with an a priori hypothesized model of task-elicited brain activity. The GLM approach is less useful than multivariate data-driven techniques for characterizing the dynamics of brain networks having coherent spatiotemporal correlation, but whose components and time courses are not known in advance. Spatial independent component analysis (ICA) [McKeown et al., 1998, 2003; Calhoun et al., 2001c, 2003] is one approach to identify groups of spatially remote brain regions that have strongly correlated patterns of neural activity change.

Because previous studies of mental chronometry reliably find concurrent activation of frontostriatal brain regions on interval timing tasks and there is some evidence for functional coupling among many of these regions, the primary objective of this study was to test the hypothesis that a frontostriatal neural network mediates mental timing. The importance of frontostriatal brain regions to mental timekeeping has been documented by numerous studies and converging lines of evidence [see review by Mattell and Meck, 2004]. Spatial ICA was used to reexamine previous fMRI data (data not shown) obtained during the performance of several tasks requiring explicit timing of motor function to auditory cues. We hypothesized that there would be evidence of functional connectivity among frontal lobe and basal ganglia structures. Secondary objectives were to identify other functionally connected neural circuits and to characterize their likely function by examining their association with different paradigm demands.

MATERIALS AND METHODS

Participants

Participants were 31 healthy screened right-handed volunteers (15 men) with a mean age of 26.1 years (SD 6.48). Participants were recruited via advertisements and word of mouth at the Olin Neuropsychiatry Research Center (Hartford, CT). Participants provided written informed consent in protocols approved by Hartford Hospital's Institutional Review Board. All research procedures were conducted in adherence to ethical standards required for human subject protection.

Experimental Design

The temporal reproduction timing paradigm will be described in detail in another publication. In brief, the paradigm included three timing tasks (sychronize, syncopate, and listen) and three rates of auditory cue presentation [1.33 Hz or a 0.75-s stimulus onset asynchrony (SOA), 0.67 Hz or 1.5-s SOA, and 0.29 Hz or 3.5-s SOA]. For synchronize, participants were instructed to time their taps to coincide as closely as possible to the onset of each auditory tone. For syncopate, participants were instructed to time their taps to occur as close as possible to the midpoint between two successive tones. The listen condition was included to give participants a respite from motor responding and to serve as a comparison timing condition without explicit motor output. During the listen condition, participants were instructed to pay attention to auditory tones, but to make no motor responses. For each task, auditory tones were presented at all three different rates. The nine different combinations of the task and rate factors were presented in blocks of 21 s.

A total of three runs (each 4 min and 27 s) were presented to each participant. The order of conditions across the three

runs was pseudorandomly distributed so that no two similar conditions followed each other. Each of three experimental sessions included all nine conditions. Each fMRI session began with a 9-s rest period during which subjects were instructed to focus on a fixation point. This was followed by a block of three of the nine experimental conditions followed by a 21-s rest period, another block of three conditions and rest, and finally the remaining three conditions and rest. Participants were instructed by screen prompts displayed continuously throughout each block. Auditory tones were 100-ms 500 Hz tones with 10-ms rise and fall times. Each 1.33 Hz block contained 28 regularly presented cues; 0.67 Hz blocks contained 14 cues; and 0.29 Hz blocks contained 6 cues. A custom visual and auditory presentation package (VAPP; http://www.psychiatry.ubc.ca/sz/nilab/software/vapp) was used to control stimuli presentation timing closely. The stimulus sequences were presented to the participant by a computer-controlled auditory sound system that delivered the auditory stimuli with earphones embedded within 30 dB sound attenuating MRI-compatible headphones. All participants reported that they could hear the stimuli and discriminate them from the background scanner noise. Prior to beginning the task, each participant performed a practice trial that included all nine conditions to ensure understanding of the instructions. A commercially available MRI-compatible fiber-optic response device (Lightwave Medical, Vancouver, Canada) was used to acquire behavioral responses. Stimulus events and behavioral responses were recorded and monitored online using a separate computer.

Imaging Parameters

Imaging was implemented on a Siemens Allegra 3T system located at the Olin Neuropsychiatry Research Center. Each participant's head was firmly secured using a custom head holder. Localizer images were acquired for use in prescribing the functional image volumes. The echo planar image (EPI) gradient-echo pulse sequence (TR/TE = 1,500/28 ms; flip angle = 65°; FOV = 24 × 24 cm; 64 × 64 matrix; 3.4 × 3.4 mm in plane resolution; 5 mm effective slice thickness; 30 slices) effectively covered the entire brain (150 mm) in 1.5 s. Head motion was restricted using a custom-built cushion inside the head coil. The three stimulus runs each consisted of 178 time points, including a 9-s rest session at the beginning that was collected to allow for T_1 effects to stabilize. These six initial images were not included in any subsequent analyses.

Image Processing

Functional images were reconstructed offline and each run was separately realigned using INRIAlign [Freire and Mangin, 2001; Freire et al., 2002] as implemented in Statistical Parametric Mapping (SPM2). Each participants' translation and rotation corrections were examined to ensure there was no excessive head motion. Corrections were less than a voxel length for all but one participant. Visual inspection of this participant's individual activation maps to a statistical model implemented in SPM2 did not reveal any obvious motion-induced artifact, so these data were retained for subsequent group analysis. A mean functional image volume was constructed for each session from the realigned image volumes. This mean image volume was then used to determine parameters for spatial normalization into Montreal Neurological Institute standardized space employed in SPM2. The normalization parameters determined for the mean functional volume were then applied to the corresponding functional image volumes for each participant. These normalized data were corrected with a custom algorithm that used linear interpolation to remove variation in BOLD signal intensity due to slice acquisition temporal onset differences. Finally, the normalized functional images were smoothed with an 8 mm full width at half-maximum (FWHM) Gaussian filter.

Independent Component Analyses

Analyses of spatiotemporal association were conducted using procedures and algorithms described in previous reports [Calhoun et al., 2001a, 2004]. In this approach, a single ICA analysis is performed on a group of participants, followed by a back reconstruction of single-subject time courses and spatial maps from the raw data. This approach includes several data compression and subject-wise data concatenation stages. This method has been shown to be a useful approach to group ICA analysis [Calhoun et al., 2001b; Schmithorst and Holland, 2004]. For computational feasibility, three principal component analysis (PCA) data reduction stages were needed. First, data from each subject were reduced from 172 to 30 dimensions. A second stage involved concatenation into groups of four subjects, each of which was reduced to 15 dimensions using PCA. This was followed by a final concatenation and reduction to 20 dimensions and independent component estimation of 20 components using a neural network algorithm that attempts to minimize the mutual information of the network outputs [Bell and Sejnowski, 1995]. Component time courses and spatial maps were then reconstructed for each subject. The resulting single-subject time course amplitudes were then calibrated (scaled) using the raw data so that they reflected percent fMRI signal strength [Calhoun et al., 2001b] and could be compared across participants. The ICA methods are available in a Group ICA of fMRI Toolbox (GIFT v1.2c) implemented in Matlab (http://icatb.sourceforge.net). The dimensionality of the data (number of components) was estimated using the minimum description length (MDL) criteria tool built into GIFT.

ICA produced 20 maximally independent patterns of spatiotemporally correlated BOLD signal changes. A systematic process was used to identify which components were retained for further analysis. The association of each component's spatial map with a priori probabilistic maps of gray matter, white matter, and cerebral spinal fluid within standardized brain space (MNI templates provided in SPM2) helped to identify those components whose patterns of correlated signal change were largely consisting of gray matter

versus nongray matter. Components with high correlation to a priori localized cerebrospinal fluid (CSF) or white matter or with low correlation to gray matter suggested they may be artifactual instead of representing hemodynamic change. Correlation analysis indicated that no component was related to the spatial distribution of white matter. Eight components were discarded because their R^2 association with CSF was greater than 0.025. An additional four components were discarded because they had less than a 0.025 R^2 association with gray matter. Visual inspection of discarded components suggested that they represented eyeball movements, head motion, and cardiac-induced pulsatile artifact at the base of the brain.

Visualization of Spatial Components

The ICA analysis produced three session-specific component spatial maps for each participant. These maps were transformed to z-scores, incorporating a bias term to center each image's distribution of z-scores at zero. Z-score maps for the three sessions were averaged to produce one component map for each participant used in the SPM2 analyses. SPM2 random-effects analyses were used on these individual subject component maps to visualize which brain regions were statistically significant for each component. The statistical significance of the results was evaluated using $P < 0.0001$ family-wise error rate [Worsley et al., 1996] correction for searching the whole brain. Previous analyses employing these methods [Calhoun et al., 2004] indicate that stringent corrected statistical thresholds are appropriate for identifying which brain regions are incorporated into each independent component. Component spatial structure was visualized by color-coded component maps overlaid on axial slices of representative brain anatomy.

Examination of Component Temporal Dynamics

The time course analysis involved parameterizing the time courses using multiple regression to provide estimates of the association between time course and experimental design. The conditions in the experiment were represented using a canonical hemodynamic response model in SPM2 [Josephs et al., 1997]. This SPM model separately represented each combination of task and rate, leaving rest blocks unmodeled. These analyses yielded R^2 values that represented the overall association of all sessions in the experimental design to each component time course. A second analysis examined the magnitude of the session mean unstandardized β-weights produced from this multiple regression. These coefficients represent the association of each experimental condition to signal change relative to global baseline. The sign of the coefficient represents positive versus negative signal change. It is important to note that true hemodynamic change may be in the opposite direction of that suggested by the signal of the β-coefficient. Coefficients for each participant were examined using a three-factor (task × rate × session) repeated-measures ANOVA using Greenhouse-Geiser corrections. Supplemental analyses tested for the presence of linear or quadratic trends across conditions, as well as posthoc analyses showing which specific conditions differed. Cortical surface renderings [Van Essen et al., 2001] and figures depicting ICA time course data were constructed for visualization of positive and negative signal change patterns. Time course data were averaged across participants for different experimental conditions for those components with significant task or rate effects. The figures depict true positive and negative signal change, determined by inspection of the mean activity of each brain regions during task performance.

Behavioral Analyses

Repeated-measures regression indicated that there were statistically significant differences in accuracy (measured as absolute deviation between the auditory cue and the response) between tasks with a motor component ($P < 0.05$) and among rates ($P < 0.001$), with accuracy differences among all three rates of synchronous and syncopated tapping. Participants were slightly more accurate during synchronization than syncopation. These data showed increased variability of timing accuracy with larger intervals, consistent with well-described effects of interval length [Wing and Kristofferson, 1973; Gibbon et al., 1997]. As discussed by Matell and Meck [2004], this scalar property of interval timing is invariant across different interval lengths and represents one basis for investigation of the neural substrates of clock or memory components of interval timing mechanisms. Behavioral performance adhering to this pattern indicates the operation of mental timekeeping as previously examined in numerous studies [see review by Matell and Meck, 2004].

RESULTS

Eight components that depicted spatiotemporal relationships within standardized brain space were identified. Brain regions in these components are listed in Table I, along with the x-, y-, and z-coordinates of the peak *t*-score within each region. An illustration of all components overlaid on a map of brain structure is displayed in Figure 1, separately color-coded for each component. Each component's overall association with the experimental paradigm is listed in Table II, in order of descending correlation (R^2) to the overall SPM2 model. Table II also lists mean and standard deviation of the participants' β-weights for each condition, extracted from the above multiple regression and Greenhouse-Geisser significance levels (*P*) for each repeated-measures ANOVA test of task, rate, or task × rate performed on those β-weights. Specific results of these tests are detailed below. No component had a significant effect of session, indicating that all three runs provided comparable data to task and rate analyses. Each of the eight components that survived our artifact rejection criteria are listed below.

Component 1

The component that showed the strongest association with the experimental design ($R^2 = 0.479$) comprised frontostriatal brain regions, including supplementary motor area, anterior cingulate gyrus, bilateral anterior insula, bilateral putamen/

TABLE I. List of brain regions within components showing significant spatiotemporal correlation

Component, color, and regions	Brodmann areas	*x, y, z*	t_{30}
1: Red			
Cingulate gyrus (RCZ)	24/32	−6, 30, 30	19.79*
Cingulate gyrus (CCZ)	24/32	−6, 9, 42	19.02*
Superior frontal gyrus (SMA)	6	3, 15, 60	15.18*
R superior/middle frontal gyrus	10	27, 48, 24	11.88*
L insula	13/47	−33, 12, 0	25.52*
R insula	13/47	33, 18, 0	23.14*
R middle temporal gyrus	21/22	66, −36, 3	11.15*
R supramarginal gyrus	40	54, −48, 33	10.64**
L caudate/putamen/globus pallidus		−15, 9, 9	21.23*
R caudate/putamen/globus pallidus		12, 6, 9	18.73*
L thalamus		12, −15, 3	15.60*
R thalamus		15, −12, 12	17.71*
2: Blue			
Superior frontal gyrus	6/8	3, 3, 63	11.10**
R superior/middle frontal gyrus	6	27, 9, 66	11.42*
L middle frontal gyrus	10/46	−42, 42, 27	12.26*
R middle frontal gyrus	9/10/46	39, 48, 21	21.00*
R inferior frontal gyrus	44/45	57, 9, 12	12.76*
R inferior parietal lobule	40	48, −39, 48	13.62*
↓ anterior cingulate (pregenual)	24/32	−3, 42, 9	27.55*
↓ medial frontal gyrus (ventral)	11	0, 45, −18	15.93*
↓ medial frontal gyrus (dorsal)	9	3, 45, 24	16.25*
↓ L middle frontal gyrus	8	−39, 18, 51	13.78*
↓ Precuneus	7	−3, −60, 30	32.53*
↓ L posterior cingulate gyrus	23/30/31	−6, −48, 9	16.31*
↓ R posterior cingulate gyrus	23/30/31	9, −51, 9	11.57*
↓ L middle/inferior temporal gyrus	20/21	−51, 3, −36	14.16*
↓ L superior temporal gyrus (posterior)	39	−51, −66, 27	20.83*
↓ R superior temporal gyrus (posterior)	39	48, −57, 24	12.10*
↓ R cerebellum (posterior lobe)		27, −87, −36	11.82*
3: Aqua			
Medial frontal gyrus (pre-SMA)	6/8	−3, 36, 42	10.99**
L middle frontal gyrus	8/9/46	−48, 12, 42	10.89**
L middle frontal gyrus	10/11	−42, 51, −3	10.56**
R middle frontal gyrus	8/9/46	48, 24, 27	13.75*
L inferior parietal lobule/supramarginal gyrus	39/40	−45, −57, 39	14.49*
R inferior parietal lobule/supramarginal gyrus	39/40	51, −57, 36	12.99*
4: Green			
Cingulate gyrus (CCZ)	24/32	3, 0, 45	10.49**
L postcentral gyrus	2/3	−54, −18, 45	13.33*
L superior temporal gyrus	22/42	−57, 3, 0	15.99*
L superior/transverse temporal gyrus	41/42	−60, −27, 9	14.74*
R superior temporal gyrus	22/42	60, 3, −3	14.51*
R superior/transverse temporal gyrus	41/42	54, −18, 9	14.07*
R cerebellum (posterior lobe)		21, −60, −24	13.19*
↓ L middle frontal gyrus	6/8	−27, 12, 51	11.47*
↓ R middle frontal gyrus	6/8	24, 30, 48	11.51*
5: Yellow			
L cuneus	18/19	−9, −93, 24	18.89*
R cuneus	18/19	15, −87, 18	19.38*
L lingual	18/19	−12, −63, −3	21.11*
R lingual	18/19	6, −75, −3	21.03*
6: Purple			
Medial frontal gyrus (SMA)	6	0, 3, 51	15.95*
L precentral gyrus	6	−48, −15, 54	13.71*
R precentral gyrus	6	45, −9, 54	15.34*
L postcentral gyrus	2/3	−42, −27, 54	19.33*
R postcentral gyrus	2/3	45, −27, 51	15.38*
Paracentral lobule		0, −39, 63	16.64*
↓ L inferior frontal gyrus	45/47	−54, 15, 3	11.61*
↓ R inferior frontal gyrus	13/47	30, 18, −9	12.83*
↓ R middle temporal gyrus	21	57, −27, −12	10.28**

TABLE I. (Continued)

Component, color, and regions	Brodmann areas	x, y, z	t_{30}
7: Pink			
R middle frontal gyrus	6	33, 3, 60	12.76*
L superior/inferior parietal lobule	7/40	−27, −63, 51	16.33*
R superior/inferior parietal lobule	7/40	33, −66, 48	17.00*
L precuneus	7	−6, −69, 51	19.58*
R precuneus	7	12, −69, 45	16.24*
↓ L inferior frontal gyrus	11/47	−48, −39, −12	9.63***
↓ R cerebellum (posterior lobe)		27, −84, −42	11.07**
8: Orange			
L cerebellum (anterior lobe)		−15, −48, −36	14.66*
L cerebellum (anterior lobe)		−3, −45, −36	15.02*
R cerebellum (posterior lobe)		21, −51, −48	12.26*

Columns depict component number (and associated color on Fig. 1), anatomical label, MNI coordinate for peak activation voxel, and *t*-score from random-effects analysis. Unless otherwise noted, regions show significant increases in hemodynamic activity. Regions noted ↓ show relative decreases in hemodynamic activity.
* $P < 0.0000001$ FWE; ** $P < 0.000001$ FWE; *** $P < 0.00001$ FWE.

globus pallidus, and bilateral thalamus. Right middle temporal gyrus, right supramarginal gyrus, and a small region of right dorsolateral prefrontal cortex were also components of this circuit. The lack of significant ANOVA differences suggests that this neural circuit was active across all tasks and rates.

Component 2

This component comprised a network of regions including the anterior cingulate, ventral medial frontal gyrus, dorsal medial frontal gyrus, precuneus, bilateral posterior cin-

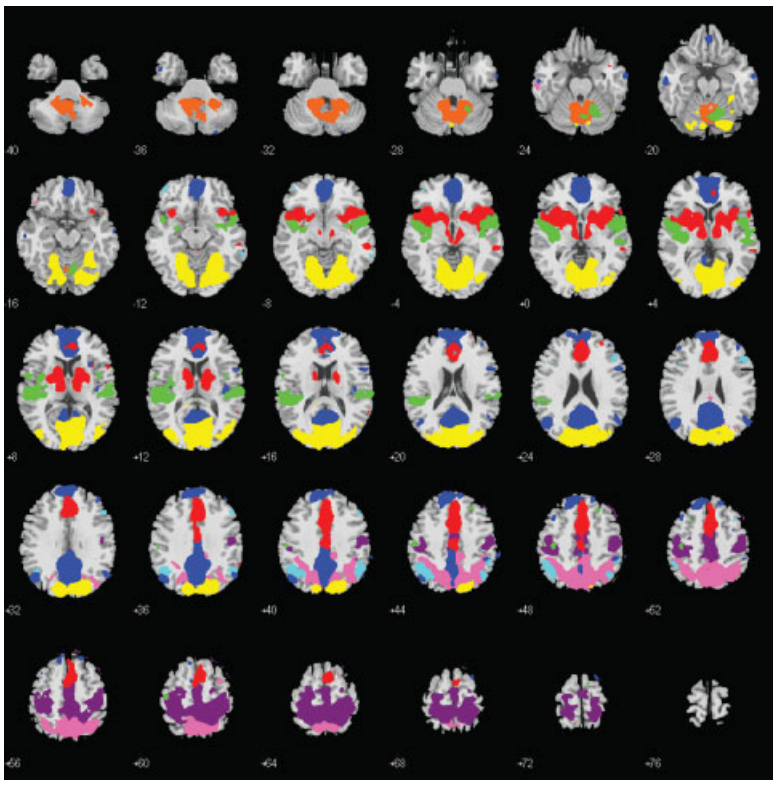

Figure 1.

Illustration of eight independent components identified in the analysis. The overlay was constructed in ascending order of R^2 association with the experimental design, with the weakest component entered first. Because there is overlap of some brain regions across components, a detailed list of what brain areas comprise each component is listed in Table I, along with a color key identifying each. All component maps are thresholded at $P < 0.000001$ FWE, corrected for searching the whole brain.

TABLE II. Results of repeated-measures ANOVA on the coefficients derived from multiple regression analysis of component time courses with paradigm design

Component	Color	Average R^2	Listen, β mean (SD)			Synchronize, β mean (SD)			Syncopate, β mean (SD)			*P**		
			1.33 Hz	0.67 Hz	0.29 Hz	1.33 Hz	0.67 Hz	0.29 Hz	1.33 Hz	0.67 Hz	0.29 Hz	Task	Rate	Task × rate
1	Red	0.479	−0.081 (0.60)	−0.256 (1.37)	0.055 (1.18)	0.077 (2.13)	0.080 (1.90)	0.038 (2.41)	0.438 (2.85)	0.108 (2.53)	−0.027 (2.31)	0.496	0.290	0.252
2	Blue	0.410	−0.037 (0.65)	−0.186 (0.71)	−0.241 (0.66)	−0.248 (0.88)	−0.676 (0.98)	−0.828 (1.14)	−0.685 (0.87)	−0.999 (1.35)	−1.085 (0.85)	< 0.001**	0.005**	0.163
3	Aqua	0.364	0.103 (0.65)	0.173 (1.31)	0.045 (0.85)	0.103 (0.62)	0.210 (0.68)	0.343 (0.85)	0.286 (0.96)	0.528 (1.45)	0.431 (1.42)	0.102	0.245	0.291
4	Green	0.357	−0.006 (0.48)	0.010 (0.27)	0.139 (0.48)	0.282 (1.44)	0.062 (0.88)	0.182 (0.92)	0.455 (1.05)	0.362 (0.79)	0.109 (0.54)	0.108	0.305	0.232
5	Yellow	0.334	−0.462 (1.26)	−0.189 (1.10)	0.009 (0.79)	−0.013 (0.59)	−0.301 (0.92)	−0.099 (0.71)	−0.200 (0.81)	−0.508 (1.11)	−0.882 (1.47)	0.039**	0.360	0.022
6	Purple	0.327	−0.116 (1.00)	−0.284 (1.85)	−0.043 (1.26)	−0.079 (0.81)	−0.034 (0.85)	−0.253 (1.18)	−0.363 (1.75)	−0.372 (1.92)	−0.491 (1.74)	0.222	0.707	0.780
7	Pink	0.205	−0.240 (1.01)	0.087 (0.60)	0.087 (0.59)	−0.157 (0.54)	−0.145 (1.17)	0.040 (0.86)	−0.075 (0.77)	0.185 (0.53)	−0.034 (0.92)	0.358	0.003**	0.534
8	Orange	0.135	0.090 (0.84)	0.101 (0.78)	−0.051 (0.40)	−0.070 (0.48)	0.108 (0.59)	−0.057 (0.74)	−0.050 (0.78)	−0.027 (0.59)	−0.018 (0.49)	0.603	0.516	0.553

Columns depict component (and associated color on Fig. 1), average overall association (R^2) of component time courses with paradigm design, participant β mean (SD), and significance levels for task, rate, and task × rate interaction conditions.

* Significance levels reflect Greenhouse-Geisser corrections for multiple comparisons from the repeated-measures ANOVA. Effects surpassing a corrected threshold of $P < 0.05$ are indicated with a double asterisk (**).

gulate gyri, and bilateral posterior superior temporal gyri. These regions showed negative signal change during experimental timing conditions. Other brain regions in this network showed positive signal change during task performance, including superior frontal gyrus (BA 6/8), right middle frontal gyrus (BA 9/46), right precentral gyrus, and right inferior parietal lobule (BA 40). ANOVA results show that condition loadings differed both by task type and by rate. There was relatively greater association of this component with more difficult tasks (i.e., synchronization and syncopation; $F_{2,30} = 15.670$; $P < 0.001$) and with slower rates ($F_{2,30} = 7.474$; $P = 0.005$). Both effects showed significantly linear change across conditions (task $F_{1,30} = 22.092$, $P < 0.001$; rate $F_{1,30} = 9.146$, $P = 0.005$). Easier tasks (mean ± SE; listen = 0.15 ± 0.08; synchronize = 0.58 ± 0.16; syncopate = 0.92 ± 0.17) and slower rates (1.33 Hz = 0.32 ± 0.11; 0.67 Hz = 0.53 ± 0.09; 0.29 Hz = 0.81 ± 0.19) showed stronger association with the component time courses. Bonferroni-corrected posthoc comparisons showed that the β-loadings for all three tasks significantly differed from each other, but only the slowest and fastest rates significantly differed. Figure 2 shows both patterns of positive and negative signal change and average ICA time courses for significantly different conditions for easier visualization.

Component 3

Task performance engaged a network of regions including dorsal medial frontal gyrus, left middle frontal gyrus in lateral premotor cortex (BA 8), left middle frontal gyrus (BA 10/11), right middle frontal gyrus (BA 9/46), and bilateral inferior parietal lobule. The lack of significant ANOVA differences suggests that this neural circuit was active across all tasks and rates.

Component 4

Regions of left postcentral gyrus, cingulate, and bilateral superior temporal gyri (BA 22/42) comprised component 3. The lack of significant ANOVA differences suggests that this neural circuit was active across all tasks and rates.

Component 5

Areas within bilateral cuneus and lingual gyri reduced their hemodynamic activity during all tasks. This relative reduction in hemodynamic activity was most apparent during syncopation tasks ($F_{2,30} = 3.529$; $P = 0.039$). Bonferroni-corrected posthoc tests showed that syncopation conditions were more strongly associated with this component than other tasks (listen = −0.21 ± 0.14; synchronize = −0.14 ± 0.09; syncopate = −0.53 ± 0.18). There also was a significant task × rate interaction ($F_{4,30} = 3.593$; $P = 0.022$), such that bilateral cuneus and lingual showed less hemodynamic activity during the slower suprasecond rates of the syncopate condition. Figure 3 shows an illustration of component spatial extent and average ICA time courses for significantly different conditions for easier visualization of condition differences.

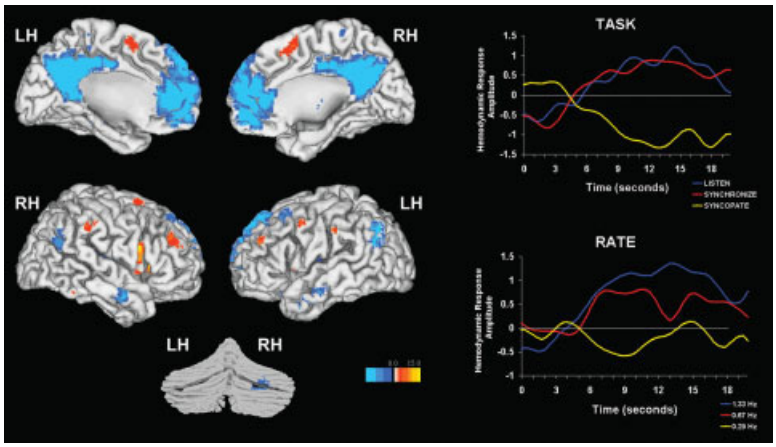

Figure 2.

Illustration of component 2 showing regions consistent with default mode network. Brain regions showing positive signal change during task performance are shown in red. Regions with true negative signal change are shown in blue. The cerebellum coronal rendering is depicted from the posterior view. Statistical results are thresholded at $P < 0.00001$ FWE, corrected for searching the whole brain. Time courses (right) for task and rate conditions depict average amplitude of the hemodynamic response for the ICA time course following start of task blocks (time 0), adjusted for other regressors in the experimental design.

Component 6

This component showed increasing activity in motor cortex regions, including supplementary motor area cortex in medial frontal gyrus, bilateral precentral gyri, bilateral postcentral gyri, and paracentral lobule. Decreasing hemodynamic activity was simultaneously observed in bilateral inferior frontal gyri and right middle temporal gyrus. Component loadings show that this neural network showed a nonsignificant tendency to greater hemodyanmic activity in motor regions during conditions requiring movement; more activity in nonmotor cortex was observed during listen.

Component 7

This component included right middle frontal gyrus (BA 6), left bilateral superior parietal lobule, and bilateral precuneus. As hemodynamic activity in these regions increased, it decreased in right inferior frontal gyrus and the right posterior lobe of the cerebellum. The ANOVA indicates that activity in these regions varied by rate of stimulus presentation ($F_{2,30} = 7.631$; $P = 0.003$). The overall association of this component β-loadings changed linearly with rate ($F_{1,30} = 13.410$; $P = 0.005$), such that the fastest rate showed negative association to the component time course (1.33 Hz = -0.16 ± 0.1), while the slowest rate had a positive association (0.29 Hz = 0.15 ± 0.12). The difference between fastest and slowest rate loadings was significantly different following Bonferroni posthoc test. Figure 4 shows both patterns of positive and negative signal change and average ICA time courses for significantly different conditions for easier visualization.

Component 8

Some activity within the cerebellum was functionally integrated, but not associated with hemodynamic activity out-

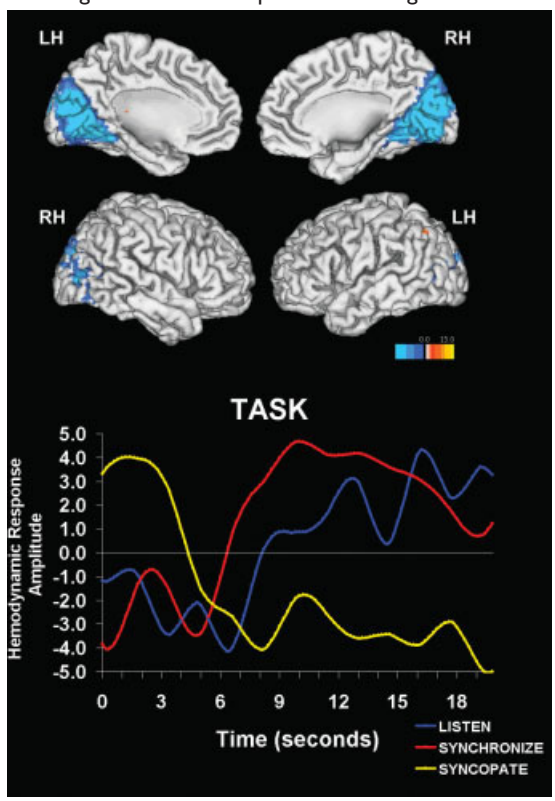

Figure 3.

Illustration of component 5 showing cortical regions that reduce hemodynamic activity during syncopation tasks (blue). Statistical results are thresholded at $P < 0.00001$ FWE, corrected for searching the whole brain. Time courses (right) for task conditions depict average amplitude of the hemodynamic response for the ICA time course following start of task blocks (time 0), adjusted for other regressors in the experimental design.

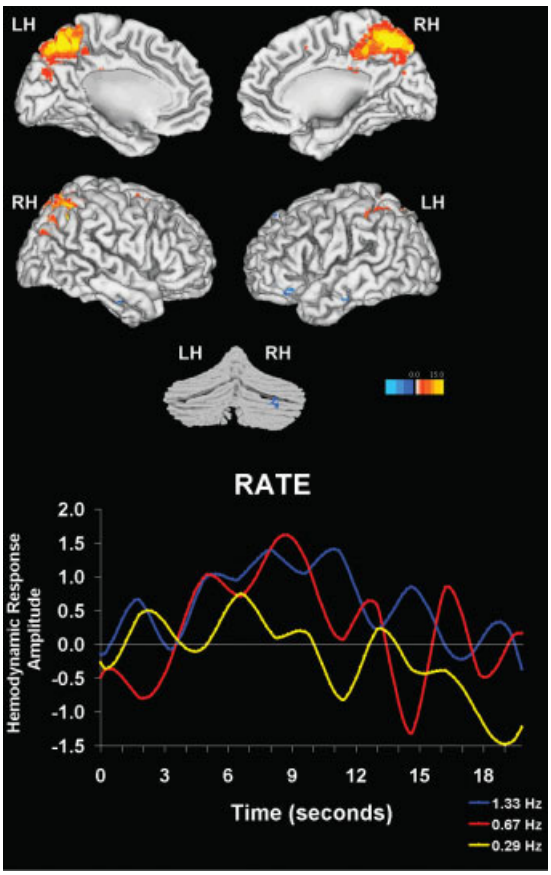

Figure 4.

Illustration of component 7 showing a frontal-parietal-cerebellar network whose activity differs between the fastest and slowest rates of stimulus presentation. Brain regions showing positive signal change during task performance are shown in red-yellow. Regions with negative signal change are shown in blue. The cerebellum coronal rendering is depicted from the posterior view. Statistical results are thresholded at $P < 0.00001$ FWE, corrected for searching the whole brain. Time courses (right) for rate conditions depict average amplitude of the hemodynamic response for the ICA time course following start of task blocks (time 0), adjusted for other regressors in the experimental design.

side the cerebellum. Areas showing significant spatiotemporal correlation included two foci in left anterior lobe and one in right posterior lobe. The lack of significant ANOVA differences suggests that this activity was present across all tasks and rates.

DISCUSSION

We examined functional connectivity during performance of tasks requiring precise mental timing of finger movements. Spatial ICA identified eight independent neural circuits with varying association to the discrete interval timing tasks used to elicit neural activity. We were careful to ensure through rigorous exclusion criteria that these components reflected patterns of brain hemodynamic activity and did not represent movement or BOLD signal artifact. The components identified in this analysis comprised brain regions found to be active in previous analyses of this data set using general linear model analytic methods (data not shown) and in previous studies of synchronized finger movements [Blinkenberg et al., 1996; Sadato et al., 1996; Lejeune et al., 1997; Rao et al., 1997; Wessel et al., 1997; Jancke et al., 1998, 2000; Menon et al., 1998; Rubia et al., 1998; Rammsayer, 1999; Kawashima et al., 2000; Macar et al., 2002; Mayville et al., 2002; Lewis and Miall, 2003; Riecker et al., 2003; Ward and Frackowiak, 2003; Hinton and Meck, 2004; Jantzen et al., 2004]. The current analysis extends those results by identifying groups of functionally integrated brain regions and relating the function of these neural circuits to particular aspects of task performance. The following discussion integrates an examination of whether these neural circuits might correspond to stages of mental timekeeping information processing models [Gibbon et al., 1984; Gibbon and Church, 1990], which include distinct clock, memory, and decision stages for the precise timing of movement.

Frontostriatal Circuit

The primary study hypothesis was that frontal lobe and basal ganglia structures would show evidence for spatiotemporal intercorrelation during the performance of discrete interval timing tasks. Consistent with this hypothesis, spatial ICA revealed a frontostriatal circuit common to all timing task conditions (component 1, red). Hemodynamic activity in bilateral caudate, putamen, and globus pallidus significantly covaried with activity in right dorsolateral prefrontal and medial supplementary motor area cortex, bilateral anterior insula, anterior cingulate, and bilateral thalamus. The component time course was the most strongly associated with the experimental paradigm, suggesting that it may be the most important neural circuit mediating performance of the timing tasks. Interestingly, this network was consistently engaged during tasks with and without explicit motor demands, which makes it unlikely that its activity merely reflects motor function. This result is most consistent with the striatal beat frequency model of interval timing proposed by Meck and colleagues, which would predict basal ganglia involvement in nonmotor timekeeping [Matell and Meck, 2000; see also Buhusi and Meck, 2005; MacDonald and Meck, 2004].

The spatial structure of this component is consistent with the well-described anatomical connections among these brain regions. These areas of prefrontal cortex are reciprocally connected to the dorsal striatum, which in turn conveys information to the globus pallidus. Globus pallidus output is relayed to the thalamus, which is widely interconnected with cortical regions, as well as back to the striatum [Mengual et al., 1999]. Anatomically derived models of basal ganglia operation have focused on the distinction between the direct corticostriatopallidal loop and an internal indirect striatopallidal pathway [Mink, 1996; Smith et al., 1998]. The direct pathway initiates movement by disinhibiting

thalamocortical input, while the indirect pathway inhibits thalamocortical output, serving to regulate jointly information flow to facilitate or inhibit particular movements or behavior. Recent evidence from comparative anatomy studies [Haber and McFarland, 2001] suggests that the thalamus may play a key role in integrating information inputs and outputs through use of oscillatory mechanisms [Steriade, 1999] that may change the dynamics of information processing in output brain regions. Therefore, the regions in this neural circuit appear suited to perform the functions of gating motor timing information via cortical inputs (i.e., direct corticostriatopallidal and indirect striatopallidal pathways) and integrating that information into temporal representations (i.e., via thalamic output pathways back to the striatum and to cortex) [Matell and Meck, 2000; Meck and Benson, 2002; MacDonald and Meck, 2004; Buhusi and Meck, 2005]. These two functions are key components of the clock stage of timing information processing models [Gibbon et al., 1984; Gibbon and Church, 1990]. Recent evidence shows that dopaminergic function modulates measures of functional connectivity in corticostriatothalamic circuits [Williams et al., 2002; Honey et al., 2003]; indeed, drugs that decrease dopaminergic function decrease the speed of the internal clock [Meck, 1986, 1996; Rammsayer, 1997, 1999]. These studies highlight the importance of this circuit in forming temporal representations.

This component also included activity within caudal anterior cingulate gyrus, supplementary motor area, bilateral anterior insula, right middle temporal gyrus, and right supramarginal gyrus. The caudal cingulate region included what has been referred to as the cingulate cognitive division (BA 24′/32′) [Devinsky et al., 1995], which recently has been further divided into a rostral cingulate and caudal cingulate zones (RCZ and CCZ, respectively) [Picard and Strick, 2001]. Previous studies suggest that the caudal aspect (CCZ) is active primarily during movement execution [Picard and Strick, 2001], whereas the rostral cingulate zone can be further subdivided into an anterior division (RCZa) important for attention to action and a posterior division (RCZp) for the selection of action [Carter et al., 2000]. Component 1 included activation throughout the anterior and posterior RCZ subdivisions. Cingulate cortex receives input from supplementary motor area, premotor, and primary motor cortex [Paus, 2001]. As previously proposed [Rubia and Smith, 2004], this suggests that the cingulate may function in this circuit to monitor and influence movement. Previous studies have linked activity in the insula to the integration of multimodal sensory signals associated with voluntary movement [Farrer and Frith, 2002]. Right parietal lobe regions also are associated with integrating sensory and motor information [Behrmann et al., 2004], particularly for movement planning [Cohen and Andersen, 2002; Assad, 2003] and prediction, perhaps also with a role for monitoring motor performance [Blakemore and Sirigu, 2003]. Indeed, this right parietal region is active during numerous previous externally paced timing tasks [Lejeune et al., 1997; Mima et al., 1999; Jancke et al., 2000; Rubia et al., 2000; Macar et al., 2002; Ward and Frackowiak, 2003; Jantzen et al., 2004]. The role of primary auditory cortex in this circuit may be to help coordinate motor activity directly with incoming auditory pacing cues. Collectively, the role of these structures may be to serve as somatosensory information input pathways to the basal ganglia and thalamus to determine and help monitor accurate movement coordination in time.

Cerebellar Circuits

The role of the cerebellum in mental timekeeping is supported by neuropsychological studies [e.g., Harrington et al., 1998] but is not yet clearly understood [Ivry and Spencer, 2004]. The current results indicate that areas of right cerebellum posterior lobe were engaged in two separate corticocerebellar neural circuits. In one network (component 4, green), an area of right cerebellum, increased activity in conjunction with activity in cingulate gyrus (CCZ), left postcentral gyrus, and bilateral superior/transverse temporal gyri. This is consistent with previous functional connectivity studies of motor function that found coordinated activity between left postcentral gyrus and right cerebellar dentate nucleus during drawing tasks [Saini et al., 2004]. Because the thalamus was not engaged in this circuit, it is likely that the cerebellum was integrated into this network through its output directly to primary motor cortex [Middleton and Strick, 1997]. The network identified here resembles the "automatic" timing system proposed by Lewis and Miall [2003]. The regions of bilateral premotor cortex (pre-PMd) [Picard and Strick, 2001] in this circuit are found in previous studies of spatial attention and working memory [Boussaoud, 2001]. As activity in bilateral lateral premotor regions decreased, activity in other brain regions increased. This is consistent with an automatic timing system that functions when attentional modulation is not required. Lewis and Miall [2003] hypothesize that automatic timing is mediated by central pattern generator mechanisms that track cellular firing rates in sensory and motor cortex, possibly with the aid of the sensory imagery or cerebellar function. Consistent with this proposal, Rao et al. [1997] observed increased hemodynamic activity in auditory cortex in the absence of auditory stimulation during a motor timing task, suggesting the brain uses sensory imagery to support motor timing. In the current experiment, strong bilateral auditory association cortex activation co-occurred with right cerebellum activity. The cerebellum might participate in this system by representing temporal aspects of sensory information, possibly by anticipating sensory events [Tesche and Karhu, 2000]. Indeed, it has been proposed that the primary function of the cerebellum in timekeeping tasks may be to provide a precise temporal representation of both motor and nonmotor tasks that require rapid and efficient execution [Ivry, 2000]. Therefore, the independence of the cerebellum from the frontostriatal timing network might reflect a reduced need to access cerebellar representations of temporal information when frontal and parietal lobe-mediated timing mechanisms are engaged. This is consistent with the idea that two separate motor timing networks may exist. Alternatively, it also

is possible that access to cerebellar temporal representations is primarily needed during motor timing on the scale of milliseconds rather than seconds, as some have proposed [Ivry and Spencer, 2004]. Future studies using different paradigm demands (e.g., temporal discrimination, rhythm reproduction, exclusively subsecond timing rates) might further clarify conditions in which the cerebellum is engaged.

In the second cerebellar network (component 7, pink), right cerebellar activity decreased in conjunction with right premotor and left inferior frontal gyrus as hemodynamic activity increased in bilateral parietal lobe regions (i.e., inferior and superior parietal lobules and precuneus). In this circuit, activity in prefrontal and cerebellum regions increased during the fastest rate of movement, but decreased during the slowest. Conversely, parietal regions showed greater activity during the slowest movement rate and decreased activity during the fastest. This connectivity is consistent with previous findings of premotor and parietal connectivity using magnetoencephalography by Pollok et al. [2006], which were attributed to evaluation of motor synchrony function. The alternation of increases and decreases in hemodyanmic activity between parietal and prefrontal cortex/cerebellum with stimulus presentation rate indicates that the cerebellum is more involved in mediating rapid coordinated movements [Ivry and Spencer, 2004], whereas parietal regions are more important for slower-paced movements. It is not clear whether rate-related differences in these parietal/prefrontal versus cerebellar regions also reflect the engagement of conscious mediation, as suggested by numerous previous neuroimaging studies [Petersen et al., 1989; Corbetta et al., 1991; Heilman et al., 1993; Winstein et al., 1997; Grafton et al., 1998; Mazoyer et al., 2002; MacDonald and Paus, 2003], but this remains a distinct possibility.

Finally, activity within the cerebellum was functionally integrated with other cerebellar regions, but this pattern of activity was not reflected in other brain areas (component 8, orange). Because this activity did not differ across task conditions, it is difficult to suggest a specific functional correlate of this activity.

Frontoparietal Circuit

Component 3 (aqua) comprised dorsolateral prefrontal and parietal lobe regions previously linked to attention and working memory functions [Fletcher and Henson, 2001] and medial frontal regions involved with processing or maintaining relevant sensory information (e.g., pre-SMA) [Picard and Strick, 2001]. Working memory representation of temporal information is an important component of information processing theories of mental timekeeping [Gibbon et al., 1984; Gibbon and Church, 1990]. Mental representations of timing intervals needed to direct motor output are believed to be stored in reference memory until a comparator mechanism evaluates whether motor activity should commence. The current results suggest that these brain regions may comprise a working memory module needed for timing operation. This interpretation is consistent with proposals made by others that the working memory function of internal clocks may involve activity within dorsolateral prefrontal cortex [Gibbon et al., 1984; Gibbon and Church, 1990; Rubia and Smith, 2004]. Previous analysis of this data set suggested that activity in some of these regions increased when longer intervals were measured (data not shown). However, the current component was unaffected by any difference in rate or task. This suggests that in addition to the rate effect previously noted in previous analyses, activity in these brain regions also may subserve a more general function required by all task conditions. One such generalized function is the short-term storage of temporal information generated by the clock stage of information processing models. Recent functional connectivity studies of working memory indicate that coordinated functional interaction among dorsolateral and ventrolateral prefrontal cortex, the premotor cortex, the intraparietal sulcus, and other subcortical regions underlies active working memory maintenance of a perceptual representation [Gazzaley et al., 2004]. Frontoparietal connectivity also has been detected using EEG coherence measures [Babiloni et al., 2004]. In that study, there was evidence for both unidirectional (i.e., parietal to frontal in beta and gamma frequencies) and bidirectional (gamma) flow of information, consistent with well-described bidirectional anatomical connections between dorsolateral and parietal cortex [Petrides, 1998].

Motor Circuits

Previous functional connectivity studies that examined motor cortex regions found significant correlation among premotor, primary motor, supplementary motor cortex in the left and right hemispheres during rest [Biswal et al., 1995; Lowe et al., 1998; Xiong et al., 1999] and correlation of sensorimotor cortex with posterior parietal association cortex and dorsal cingulate gyrus [Xiong et al., 1999]. A handful of studies have used spatial ICA to extend these results during rest [van de Ven et al., 2004] or during motor task performance [Moritz et al., 2000, 2005]. In these latter studies, only self-paced tapping engaged supplementary motor area cortex with the motor circuit [Moritz et al., 2005]. Our results (component 6, purple) extend these findings by showing functional correction of sensorimotor cortex with bilateral precentral gyri and postcentral gyri, dorsal medial frontal gyrus (i.e., supplementary motor area cortex), and the paracentral lobule. These regions may be responsible for the preparation and execution of movements, as supplementary motor and premotor cortex project to primary motor cortex [Picard and Strick, 2001]. The functional significance of increases in motor region activity with concurrent decreases in bilateral inferior frontal gyri and right middle temporal gyrus is not immediately clear. It is possible that motor timing, which requires continual engaging and disengaging motor activity, may be accompanied by diminished activity in regions known to be engaged during response inhibition [Kiehl et al., 2000]. Alternatively, others have demonstrated that right inferior frontal cortex may be active during perceptive time estimation cognitive processes, as activation of this region can occur in response to

rhythm monitoring when no motor function is required [Gruber et al., 2000; Schubotz et al., 2000]. Therefore, the inclusion of bilateral inferior frontal gyri in this neural circuit may be more related to movement monitoring and planning cognitive processes than to execution.

Other Circuits

Two components reflected systematic hemodynamic decreases during task performance. Component 2 (blue) reflects a network of brain regions frequently described as comprising a "default mode" [Gusnard et al., 2001; Raichle et al., 2001], where the degree of hemodynamic decrease may represent the brain engaging more neural resources when faced with greater task difficulty. Consistent with this interpretation, greater hemodynamic decreases were seen in tasks believed to impose greater cognitive processing demands (i.e., during motor syncopation and slower rates). As activity in these regions decreased, activity in dorsolateral prefrontal and right inferior parietal lobule increased. This provides concrete evidence for a tightly coupled relationship between activity in brain regions mediating working memory and attention with proposed default mode network regions that reduce metabolic demands. Previous analysis of this data set did not find a significant rate effect for "deactivation" in these brain regions. However, this may be because posthoc tests found that there only were significant differences between the fastest and slowest rates in the current analysis. Interestingly, this circuit was distinct from component 5 (yellow), in which bilateral cuneus and lingual gyri showed hemodynamic decreases during syncopated finger tapping. It is possible that visual cortex "deactivation" is functionally independent from hemodynamic decreases in midline medial frontal gyrus, precuneus, and posterior cingulate structures observed in previous default mode network studies. However, it is more likely that this finding represents an effect specific to syncopation performance.

Summary and Limitations

Although we identified several separate functionally integrated neural networks, we did not examine how changes in one neural circuit's activity might modulate activity in another. Using known anatomical pathways, it is possible to speculate on how information might flow in these circuits. Auditory information from primary motor cortex appears to be directly coupled to a frontostriatal timing network that integrates sensory and proprioceptive information into basal ganglia regions and the thalamus to form temporal representations [Buhusi and Meck, 2005]. Auditory information from sensory association cortex, motor activity from left primary motor cortex, and right cerebellum output might project to rostral anterior cingulate and perhaps serves to track cellular firing rates to form a secondary neural network representing timing [Paus, 2001; Lewis and Miall, 2003]. Our data suggest that temporal information output from the frontostriatal circuit is likely maintained online to guide behavior in a neural circuit that includes pre-SMA, dorsolateral prefrontal, and bilateral parietal cortex. Motor execution is subserved by a network of SMA, premotor and primary motor cortex [Picard and Strick, 2001]. It is not immediately clear exactly how the timing or working memory circuits may signal the onset of finger movements subserved by this circuit, but signaling through the SMA is a likely possibility [Picard and Strick, 2001]. The current results could be extended in future studies by using causal dynamic modeling techniques [e.g., Rajapakse et al., 2006] to test the effective connectivity among structures in each neural circuit. This might clarify how activity in these circuits may correspond to hypothetical stages of timekeeping information processing models.

Our experiment was not designed to relate behavioral performance to component structure. The analyses also were not designed to test predictions explicitly regarding particular theoretical stages of information processing or distributed models of temporal processing [Ivry and Spencer, 2004; Buhusi and Meck, 2005; Lustig et al., 2005]. However, the analysis produced results consistent with aspects of both models. We note that component 1 not only appears suited to perform clock functions, it integrates these brain regions with others that may reflect timing task performance monitoring. This distributed circuit is more complex than that hypothesized in strict localizationist information processing models of mental timekeeping. A frontoparietal circuit (component 3) also was identified that may correspond to the working memory stage of timing information processing models. Like the frontostriatal circuit, this distributed network was active during all timing task components, suggesting a ubiquitous importance of activity in these brain regions for mental timing. It is noted that the analysis did not produce a component suggestive of the proposed "decision" stage of mental timekeeping models. If such a network exists, it might be hypothesized to include anterior cingulate, dorsolateral prefrontal, and premotor cortex. Indeed, one previous study shows that decision-making in uncertain situations involves an integrated network including anterior cingulate, lateral prefrontal and parietal cortex, and the striatum [Cohen et al., 2005]. The current paradigm, in which continual motor output was necessary in two of the three tasks types, may not have had an independent pattern of activity underlying the decision stage. Decision-making function likely was integrated into the frontostriatal and/or frontoparietal circuits. It is possible that a separate decision stage neural circuit might be found in a temporal discrimination or estimation task more ideally suited to reflect decision-making operations. It also is important to note that the distributed nature of the neural circuits crucial for interval timing suggests that the search for specific information processing modules may be arbitrary. Numerous cognitive processes appear subsumed into the function of each functional circuit, as demonstrated by the breadth of regions in each component and by the significant association between several component time courses and multiple aspects of interval timing tasks (e.g., rate, task). Indeed, recent proposals for distributed coincidence detection models of interval timing [Ivry and Spencer, 2004; Buhusi and Meck, 2005; Lustig et

al., 2005] hold great promise for characterizing how specific neural mechanisms may underlie the functional connections among brain regions in each circuit engaged for complex information processing.

As noted above, the network of frontostriatal brain structures is anatomically consistent with gating and neural accumulator components of the clock stage of temporal information processing models. However, some of these brain regions also have been implicated in attentional set switching [Dreher and Grafman, 2002; Dreher et al., 2002; Rushworth et al., 2002]. While it is plausible that attentional switching may contribute to neural activity at the beginning of task blocks, it is unlikely that such activity would continue throughout an extended period of timed movement. However, because the current paradigm was not constructed to differentiate the effects of switching among different instructional sets from timing neural function, additional work is needed to dissociate these cognitive processes in these brain regions.

Finally, although several different types of timing task demands were contrasted in the paradigm, timing neural function can be measured with other, qualitatively different types of tasks. Because this is the first fMRI study of mental timekeeping temporal dynamics, it remains to be seen whether similar results will be obtained from a functional connectivity study of temporal discrimination, or from a timing task that is less cognitively demanding. Indeed, Pollok et al. [2006] suggest that the lower complexity of their auditory paced finger-tapping task may be a factor in why basal ganglia activity was not observed in their neural circuit. Additional work with these various task types is needed before neural network models of mental timekeeping can be fully characterized.

This study used a novel analytic technique to provide evidence supporting the existence of a frontostriatal timing neural network and demonstrated its importance to the performance of discrete interval timing tasks. This network comprises distributed brain structures that are anatomically consistent with the proposed mental clock functions of information processing timekeeping models. Several other distinct neural circuits also were identified, including a possible alternative timing neural network consistent with previously proposed automatic timing systems. Future studies of neural timekeeping functional connectivity should attempt to determine the exact function of this circuit by examining its function in different types of timing tasks. Another neural network was identified that may reflect the brain regions important to the working memory stage of timing models. The association between these networks and their presumed function within these models remains to be explicitly tested.

REFERENCES

Assad JA (2003): Neural coding of behavioral relevance in parietal cortex. Curr Opin Neurobiol 13:194–197.

Babiloni C, Babiloni F, Carducci F, Cincotti F, Vecchio F, Cola B, Rossi S, Miniussi C, Rossini PM (2004): Functional frontoparietal connectivity during short-term memory as revealed by high-resolution EEG coherence analysis. Behav Neurosci 118:687–697.

Behrmann M, Geng JJ, Shomstein S (2004): Parietal cortex and attention. Curr Opin Neurobiol 14:212–217.

Bell AJ, Sejnowski TJ (1995): An information-maximization approach to blind separation and blind deconvolution. Neural Comput 7:1129–1159.

Biswal B, Yetkin FZ, Haughton VM, Hyde JS (1995): Functional connectivity in the motor cortex of resting human brain using echo-planar MRI. Magn Reson Med 34:537–541.

Blakemore SJ, Sirigu A (2003): Action prediction in the cerebellum and in the parietal lobe. Exp Brain Res 153:239–245.

Blinkenberg M, Bonde C, Holm S, Svarer C, Andersen J, Paulson OB, Law I (1996): Rate dependence of regional cerebral activation during performance of a repetitive motor task: a PET study. J Cereb Blood Flow Metab 16:794–803.

Boussaoud D (2001): Attention versus intention in the primate premotor cortex. Neuroimage 14(1 Pt 2):S40–S45.

Buhusi CV, Meck WH (2005): What makes us tick? functional and neural mechanisms of interval timing. Nat Rev Neurosci 6:755–765.

Calhoun VD, Adali T, McGinty VB, Pekar JJ, Watson TD, Pearlson GD (2001a): fMRI activation in a visual-perception task: network of areas detected using the general linear model and independent components analysis. Neuroimage 14:1080–1088.

Calhoun VD, Adali T, Pearlson GD, Pekar JJ (2001b): A method for making group inferences from functional MRI data using independent component analysis. Hum Brain Mapp 14:140–151.

Calhoun VD, Adali T, Pearlson GD, Pekar JJ (2001c): Spatial and temporal independent component analysis of functional MRI data containing a pair of task-related waveforms. Hum Brain Mapp 13:43–53.

Calhoun VD, Adali T, Hansen JC, Larsen J, Pekar JJ (2003): ICA of fMRI: an overview. Nara, Japan: Proceedings of the International Conference on ICA and BSS.

Calhoun VD, Pekar JJ, Pearlson GD (2004): Alcohol intoxication effects on simulated driving: exploring alcohol-dose effects on brain activation using functional MRI. Neuropsychopharmacology 29:2097–2017.

Carter CS, Macdonald AM, Botvinick M, Ross LL, Stenger VA, Noll D, Cohen JD (2000): Parsing executive processes: strategic vs. evaluative functions of the anterior cingulate cortex. Proc Natl Acad Sci USA 97:1944–1948.

Cohen YE, Andersen RA (2002): A common reference frame for movement plans in the posterior parietal cortex. Nat Rev Neurosci 3:553–562.

Cohen MX, Heller AS, Ranganath C (2005): Functional connectivity with anterior cingulate and orbitofrontal cortices during decision-making. Brain Res Cogn Brain Res 23:61–70.

Corbetta M, Miezin FM, Dobmeyer S, Shulman GL, Petersen SE (1991): Selective and divided attention during visual discriminations of shape, color, and speed: functional anatomy by positron emission tomography. J Neurosci 11:2383–2402.

Coull JT, Vidal F, Nazarian B, Macar F (2004): Functional anatomy of the attentional modulation of time estimation. Science 303: 1506–1508.

Devinsky O, Morrell MJ, Vogt BA (1995): Contributions of anterior cingulate cortex to behaviour. Brain 118(Pt 1):279–306.

Dreher JC, Grafman J (2002): The roles of the cerebellum and basal ganglia in timing and error prediction. Eur J Neurosci 16:1609–1619.

Dreher JC, Koechlin E, Ali SO, Grafman J (2002): The roles of timing and task order during task switching. Neuroimage 17:95–109.

Farrer C, Frith CD (2002): Experiencing oneself vs another person as being the cause of an action: the neural correlates of the experience of agency. Neuroimage 15:596–603.

Ferrandez AM, Hugueville L, Lehericy S, Poline JB, Marsault C, Pouthas V (2003): Basal ganglia and supplementary motor area subtend duration perception: an fMRI study. Neuroimage 19: 1532–1544.

Fletcher PC, Henson RN (2001): Frontal lobes and human memory: insights from functional neuroimaging. Brain 124(Pt 5):849–881.

Freire L, Mangin JF (2001): Motion correction algorithms may create spurious brain activations in the absence of subject motion. Neuroimage 14:709–722.

Freire L, Roche A, Mangin JF (2002): What is the best similarity measure for motion correction in fMRI time series? IEEE Trans Med Imaging 21:470–484.

Friston KJ, Frith CD, Turner R, Frackowiak RS (1995): Characterizing evoked hemodynamics with fMRI. Neuroimage 2:157–165.

Gazzaley A, Rissman J, Desposito M (2004): Functional connectivity during working memory maintenance. Cogn Affect Behav Neurosci 4:580–599.

Gibbon J, Church RM, Meck WH (1984): Scalar timing in memory. Ann NY Acad Sci 423:52–77.

Gibbon J, Church RM (1990): Representation of time. Cognition 37:23–54.

Gibbon J, Malapani C, Dale CL, Gallistel C (1997): Toward a neurobiology of temporal cognition: advances and challenges. Curr Opin Neurobiol 7:170–184.

Grafton ST, Fagg AH, Arbib MA (1998): Dorsal premotor cortex and conditional movement selection: a PET functional mapping study. J Neurophysiol 79:1092–1097.

Gruber O, Kleinschmidt A, Binkofski F, Steinmetz H, von Cramon DY (2000): Cerebral correlates of working memory for temporal information. Neuroreport 11:1689–1693.

Gusnard DA, Akbudak E, Shulman GL, Raichle ME (2001): Medial prefrontal cortex and self-referential mental activity: relation to a default mode of brain function. Proc Natl Acad Sci USA 98:4259–4264.

Haber S, McFarland NR (2001): The place of the thalamus in frontal cortical-basal ganglia circuits. Neuroscientist 7:315–324.

Harrington DL, Lee RR, Boyd LA, Rapcsak SZ, Knight RT (2004): Does the representation of time depend on the cerebellum? Effect of cerebellar stroke. Brain 127(Pt 3):561–574.

Heilman KM, Bowers D, Valenstein E, Watson RT (1993): Disorders of visual attention. Baillieres Clin Neurol 2:389–413.

Hinton SC, Meck WH (2004): Frontal-striatal circuitry activated by human peak-interval timing in the supra-seconds range. Brain Res Cogn Brain Res 21:171–182.

Honey GD, Suckling J, Zelaya F, Long C, Routledge C, Jackson S, Ng V, Fletcher PC, Williams SC, Brown J, et al. (2003): Dopaminergic drug effects on physiological connectivity in a human cortico-striato-thalamic system. Brain 126(Pt 8):1767–1781.

Ivry R (2000): Exploring the role of the cerebellum in sensory anticipation and timing: commentary on Tesche and Karhu. Hum Brain Mapp 9:115–118.

Ivry RB, Spencer RM (2004): The neural representation of time. Curr Opin Neurobiol 14:225–232.

Jancke L, Specht K, Mirzazade S, Loose R, Himmelbach M, Lutz K, Shah NJ (1998): A parametric analysis of the "rate effect" in the sensorimotor cortex: a functional magnetic resonance imaging analysis in human subjects. Neurosci Lett 252:37–40.

Jancke L, Loose R, Lutz K, Specht K, Shah NJ (2000): Cortical activations during paced finger-tapping applying visual and auditory pacing stimuli. Brain Res Cogn Brain Res 10:51–66.

Jantzen KJ, Steinberg FL, Kelso JA (2004): Brain networks underlying human timing behavior are influenced by prior context. Proc Natl Acad Sci USA 101:6815–6820.

Josephs O, Turner R, Friston K (1997): Event-related fMRI. Hum Brain Mapp 5:243–248.

Kawashima R, Okuda J, Umetsu A, Sugiura M, Inoue K, Suzuki K, Tabuchi M, Tsukiura T, Narayan SL, Nagasaka T, et al. (2000): Human cerebellum plays an important role in memory-timed finger movement: an fMRI study. J Neurophysiol 83:1079–1087.

Kiehl KA, Liddle PF, Hopfinger JB (2000): Error processing and the rostral anterior cingulate: an event-related fMRI study. Psychophysiology 37:216–223.

Lejeune H, Maquet P, Bonnet M, Casini L, Ferrara A, Macar F, Pouthas V, Timsit-Berthier M, Vidal F (1997): The basic pattern of activation in motor and sensory temporal tasks: positron emission tomography data. Neurosci Lett 235:21–24.

Lewis PA, Miall RC (2003): Distinct systems for automatic and cognitively controlled time measurement: evidence from neuroimaging. Curr Opin Neurobiol 13:250–255.

Lowe MJ, Mock BJ, Sorenson JA (1998): Functional connectivity in single and multislice echoplanar imaging using resting-state fluctuations. Neuroimage 7:119–132.

Lustig C, Matell MS, Meck WH (2005): Not "just" a coincidence: frontal-striatal interactions in working memory and interval timing. Memory 13:441–448.

Macar F, Lejeune H, Bonnet M, Ferrara A, Pouthas V, Vidal F, Maquet P (2002): Activation of the supplementary motor area and of attentional networks during temporal processing. Exp Brain Res 142:475–485.

MacDonald CJ, Meck WH (2004): Systems-level integration of interval timing and reaction time. Neurosci Biobehav Rev 28:747–769.

MacDonald PA, Paus T (2003): The role of parietal cortex in awareness of self-generated movements: a transcranial magnetic stimulation study. Cereb Cortex 13:962–967.

Matell MS, Meck WH (2000): Neuropsychological mechanisms of interval timing behavior. Bioessays 22:94–103.

Matell MS, Meck WH (2004): Cortico-striatal circuits and interval timing: coincidence detection of oscillatory processes. Brain Res Cogn Brain Res 21:139–170.

Mayville JM, Jantzen KJ, Fuchs A, Steinberg FL, Kelso JA (2002): Cortical and subcortical networks underlying syncopated and synchronized coordination revealed using fMRI. Functional magnetic resonance imaging. Hum Brain Mapp 17:214–229.

Mazoyer P, Wicker B, Fonlupt P (2002): A neural network elicited by parametric manipulation of the attention load. Neuroreport 13: 2331–2334.

McKeown MJ, Makeig S, Brown GG, Jung TP, Kindermann SS, Bell AJ, Sejnowski TJ (1998): Analysis of fMRI data by blind separation into independent spatial components. Hum Brain Mapp 6:160–188.

McKeown MJ, Hansen LK, Sejnowsk TJ (2003): Independent component analysis of functional MRI: what is signal and what is noise? Curr Opin Neurobiol 13:620–629.

Meck WH (1986): Affinity for the dopamine D2 receptor predicts neuroleptic potency in decreasing the speed of an internal clock. Pharmacol Biochem Behav 25:1185–1189.

Meck WH (1996): Neuropharmacology of timing and time perception. Brain Res Cogn Brain Res 3:227–242.

Meck WH, Benson AM (2002): Dissecting the brain's internal clock: how frontal-striatal circuitry keeps time and shifts attention. Brain Cogn 48:195–211.

Meck WH, Malapani C (2004): Neuroimaging of interval timing. Brain Res Cogn Brain Res 21:133–137.

Mengual E, de las Heras S, Erro E, Lanciego JL, Gimenez-Amaya JM (1999): Thalamic interaction between the input and the output systems of the basal ganglia. J Chem Neuroanat 16:187–200.

Menon V, Glover GH, Pfefferbaum A (1998): Differential activation of dorsal basal ganglia during externally and self paced sequences of arm movements. Neuroreport 9:1567–1573.

Menon V, Anagnoson RT, Glover GH, Pfefferbaum A (2000): Basal ganglia involvement in memory-guided movement sequencing. Neuroreport 11:3641–3645.

Middleton FA, Strick PL (1997): Cerebellar output channels. Int Rev Neurobiol 41:61–82.

Mima T, Sadato N, Yazawa S, Hanakawa T, Fukuyama H, Yonekura Y, Shibasaki H (1999): Brain structures related to active and passive finger movements in man. Brain 122(Pt 10):1989–1997.

Mink JW (1996): The basal ganglia: focused selection and inhibition of competing motor programs. Prog Neurobiol 50:381–425.

Moritz CH, Haughton VM, Cordes D, Quigley M, Meyerand ME (2000): Whole-brain functional MR imaging activation from a finger-tapping task examined with independent component analysis. Am J Neuroradiol 21:1629–1635.

Moritz CH, Carew JD, McMillan AB, Meyerand ME (2005): Independent component analysis applied to self-paced functional MR imaging paradigms. Neuroimage 25:181–192.

Paus T (2001): Primate anterior cingulate cortex: where motor control, drive and cognition interface. Nat Rev Neurosci 2:417–424.

Petersen SE, Robinson DL, Currie JN (1989): Influences of lesions of parietal cortex on visual spatial attention in humans. Exp Brain Res 76:267–280.

Petrides M (1998): Specialized systems for the processing of mnemonic information within the primate frontal cortex. In: Roberts AC, Robbins TW, Weiskrantz L, editors. The Prefrontal Cortex: Executive and Cognitive Functions. Oxford: Oxford University Press. p 103–116.

Picard N, Strick PL (2001): Imaging the premotor areas. Curr Opin Neurobiol 11:663–672.

Pollok B, Gross J, Schnitzler A (2006): How the brain controls repetitive finger movements. J Physiol Paris 99:8–13.

Pouthas V, George N, Poline JB, Pfeuty M, Vandemoorteele PF, Hugueville L, Ferrandez AM, Lehericy S, Lebihan D, Renault B (2005): Neural network involved in time perception: an fMRI study comparing long and short interval estimation. Hum Brain Mapp 25:433–441.

Raichle ME, MacLeod AM, Snyder AZ, Powers WJ, Gusnard DA, Shulman GL (2001): A default mode of brain function. Proc Natl Acad Sci USA 98:676–682.

Rajapakse JC, Tan CL, Zheng X, Mukhopadhyay S, Yang K (2006): Exploratory analysis of brain connectivity with ICA. IEEE Engineer Med Biol Mag 25:102–111.

Rammsayer TH (1997): Effects of body core temperature and brain dopamine activity on timing processes in humans. Biol Psychol 46:169–192.

Rammsayer TH (1999): Neuropharmacological evidence for different timing mechanisms in humans. Q J Exp Psychol B 52:273–286.

Rao SM, Harrington DL, Haaland KY, Bobholz JA, Cox RW, Binder JR (1997): Distributed neural systems underlying the timing of movements. J Neurosci 17:5528–5535.

Riecker A, Wildgruber D, Mathiak K, Grodd W, Ackermann H (2003): Parametric analysis of rate-dependent hemodynamic response functions of cortical and subcortical brain structures during auditorily cued finger tapping: a fMRI study. Neuroimage 18:731–739.

Rubia K, Overmeyer S, Taylor E, Brammer M, Williams S, Simmons A, Andrew C, Bullmore E (1998): Prefrontal involvement in "temporal bridging" and timing movement. Neuropsychologia 36:1283–1293.

Rubia K, Overmeyer S, Taylor E, Brammer M, Williams SC, Simmons A, Andrew C, Bullmore ET (2000): Functional frontalisation with age: mapping neurodevelopmental trajectories with fMRI. Neurosci Biobehav Rev 24:13–19.

Rubia K, Smith A (2004): The neural correlates of cognitive time management: a review. Acta Neurobiol Exp (Wars) 64:329–340.

Rushworth MF, Hadland KA, Paus T, Sipila PK (2002): Role of the human medial frontal cortex in task switching: a combined fMRI and TMS study. J Neurophysiol 87:2577–2592.

Sadato N, Ibanez V, Deiber MP, Campbell G, Leonardo M, Hallett M (1996): Frequency-dependent changes of regional cerebral blood flow during finger movements. J Cereb Blood Flow Metab 16: 23–33.

Saini S, DeStefano N, Smith S, Guidi L, Amato MP, Federico A, Matthews PM (2004): Altered cerebellar functional connectivity mediates potential adaptive plasticity in patients with multiple sclerosis. J Neurol Neurosurg Psychiatry 75:840–846.

Schmithorst VJ, Holland SK (2004): Comparison of three methods for generating group statistical inferences from independent component analysis of functional magnetic resonance imaging data. J Magn Reson Imaging 19:365–368.

Schubotz RI, Friederici AD, von Cramon DY (2000): Time perception and motor timing: a common cortical and subcortical basis revealed by fMRI. Neuroimage 11:1–12.

Smith Y, Shink E, Sidibe M (1998): Neuronal circuitry and synaptic connectivity of the basal ganglia. Neurosurg Clin N Am 9:203–222.

Steriade M (1999): Coherent oscillations and short-term plasticity in corticothalamic networks. Trends Neurosci 22:337–345.

Tesche CD, Karhu JJ (2000): Anticipatory cerebellar responses during somatosensory omission in man. Hum Brain Mapp 9:119–142.

van de Ven VG, Formisano E, Prvulovic D, Roeder CH, Linden DE (2004): Functional connectivity as revealed by spatial independent component analysis of fMRI measurements during rest. Hum Brain Mapp 22:165–178.

Van Essen DC, Drury HA, Dickson J, Harwell J, Hanlon D, Anderson CH (2001): An integrated software suite for surface-based analyses of cerebral cortex. J Am Med Inform Assoc 8:443–459.

Ward NS, Frackowiak RS (2003): Age-related changes in the neural correlates of motor performance. Brain 126(Pt 4):873–888.

Wessel K, Zeffiro T, Toro C, Hallett M (1997): Self-paced versus metronome-paced finger movements: a positron emission tomography study. J Neuroimaging 7:145–151.

Williams D, Tijssen M, Van Bruggen G, Bosch A, Insola A, Di Lazzaro V, Mazzone P, Oliviero A, Quartarone A, Speelman H, et al. (2002): Dopamine-dependent changes in the functional connectivity between basal ganglia and cerebral cortex in humans. Brain 125(Pt 7):1558–1569.

Wing A, Kristofferson A (1973): Response delays and the timing of discrete motor responses. Percept Psychophys 14:5–12.

Winstein CJ, Grafton ST, Pohl PS (1997): Motor task difficulty and brain activity: investigation of goal-directed reciprocal aiming using positron emission tomography. J Neurophysiol 77:1581–1594.

Worsley KJ, Marrett S, Neelin P, Vandal AC, Friston KJ, Evans AC (1996): A unified statistical approach for determining significant voxels in images of cerebral activation. Hum Brain Mapp 4:58–73.

Xiong J, Parsons LM, Gao JH, Fox PT (1999): Interregional connectivity to primary motor cortex revealed using MRI resting state images. Hum Brain Mapp 8:151–156.